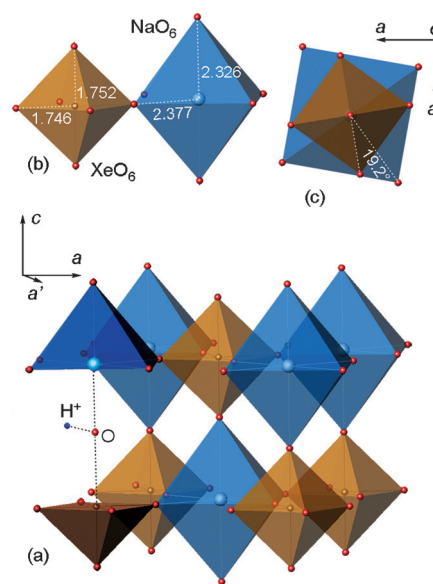


# Perovskites with the Framework-Forming Xenon

Sergey N. Britvin,\* Sergei A. Kashtanov, Maria G. Krzhizhanovskaya, Andrey A. Gurinov, Oleg V. Glumov, Stanislav Strekopytov, Yury L. Kretser, Anatoly N. Zaitsev, Nikita V. Chukanov, and Sergey V. Krivovichev

**Abstract:** The Group 18 elements (noble gases) were the last ones in the periodic system to have not been encountered in perovskite structures. We herein report the synthesis of a new group of double perovskites  $KM(XeNaO_6)$  ( $M = Ca, Sr, Ba$ ) containing framework-forming xenon. The structures of the new compounds, like other double perovskites, are built up of the alternating sequence of corner-sharing ( $XeO_6$ ) and ( $NaO_6$ ) octahedra arranged in a three-dimensional rocksalt order. The fact that xenon can be incorporated into the perovskite structure provides new insights into the problem of Xe depletion in the atmosphere. Since octahedrally coordinated  $Xe^{VIII}$  and  $Si^{IV}$  exhibit close values of ionic radii (0.48 and 0.40 Å, respectively), one could assume that  $Xe^{VIII}$  can be incorporated into hyperbaric frameworks such as  $MgSiO_3$  perovskite. The ability of Xe to form stable inorganic frameworks can further extend the rich and still enigmatic chemistry of this noble gas.

Recent discoveries in the chemistry of xenon demonstrate that there are many challenging features of this noble gas which were obscured and require further investigations.<sup>[1]</sup> Herein, we report that octavalent xenon can behave as a framework-forming element in inorganic compounds, based on the studies of a new family of double perovskites  $KM(XeNaO_6)$  where  $M = Ca, Sr, Ba$ . Perovskite structures are capable of accommodating the majority of the chemical elements;<sup>[2]</sup> however, perovskites containing noble gases in the framework have not yet been encountered. The frameworks of the synthesized Xe-perovskites, like other double perovskites  $AA'BB'O_6$ ,<sup>[3]</sup> are built up of the alternating sequence of corner-sharing ( $XeO_6$ ) and ( $NaO_6$ ) octahedra arranged in a three-dimensional rocksalt order typical for



**Figure 1.** Tetragonally distorted double perovskite framework of  $KCa(XeNaO_6)$ . a) Ordered alternation of corner-sharing  $XeO_6$  and  $NaO_6$  octahedra. The left side depicts the schematic position of proton residing in the vicinity of the oxygen site. b) Geometry of  $XeO_6$  and  $NaO_6$  octahedra. c) Relative tilt between  $XeO_6$  and  $NaO_6$  octahedra around the four-fold axis. Potassium and calcium atoms have been omitted for clarity.

double perovskites (Figure 1). The coexistence of  $Xe^{VIII}$  and  $Na(I)$  in the same framework corroborates with the known high rigidity of the perovskite structure, which can tolerate the highest possible framework charge difference (7 charge units), and rather large difference of ionic radii between  $Xe^{8+}$  (0.48 Å) and  $Na^+$  (1.02 Å).<sup>[4]</sup> The disordered potassium and alkaline earth cations occupy twelve-coordinated A-sites of the perovskite structure and play the role of the counterions balancing the negative framework charge.

Large differences between crystal ionic radii of Ca, Sr, and Ba result in the expected deviations from the cubic perovskite lattice symmetry following the respective Goldschmidt's tolerance factors.<sup>[6]</sup> whilst  $KBa(XeNaO_6)$  and  $KSr(XeNaO_6)$  exhibit undistorted cubic symmetry,  $KCa(XeNaO_6)$  demonstrates distinct tetragonal distortion<sup>[5]</sup> (Figure 2, Table 1).

The closer inspection of  $^{129}Xe$  MAS NMR spectra (Figure 3) reveals further structural features of the studied perovskites. At first, the  $^{129}Xe$  resonances corresponding to the first coordination shell of Xe (xenon-oxygen bonds in the  $XeO_6$  octahedra) are significantly broadened for all the three compounds. The comparable degree of broadening has been

[\*] Prof. S. N. Britvin, Dr. M. G. Krzhizhanovskaya, Dr. A. A. Gurinov, Dr. O. V. Glumov, Prof. A. N. Zaitsev, Prof. S. V. Krivovichev  
Saint-Petersburg State University  
Universitetskaya Nab. 7/9, 199034 St. Petersburg (Russia)  
E-mail: sergei.britvin@spbu.ru

Dr. S. A. Kashtanov, Prof. N. V. Chukanov  
Institute of Problems of Chemical Physics RAS  
142432 Chernogolovka (Russia)

Dr. S. Strekopytov  
Natural History Museum  
Cromwell Road, London SW7 5BD (UK)

Dr. Y. L. Kretser  
V.G. Khlopin Radium Institute  
2nd Murinskiy Ave. 28, 194021 St. Petersburg (Russia)

Supporting information and ORCID(s) from the author(s) for this article are available on the WWW under <http://dx.doi.org/10.1002/anie.201506690>.

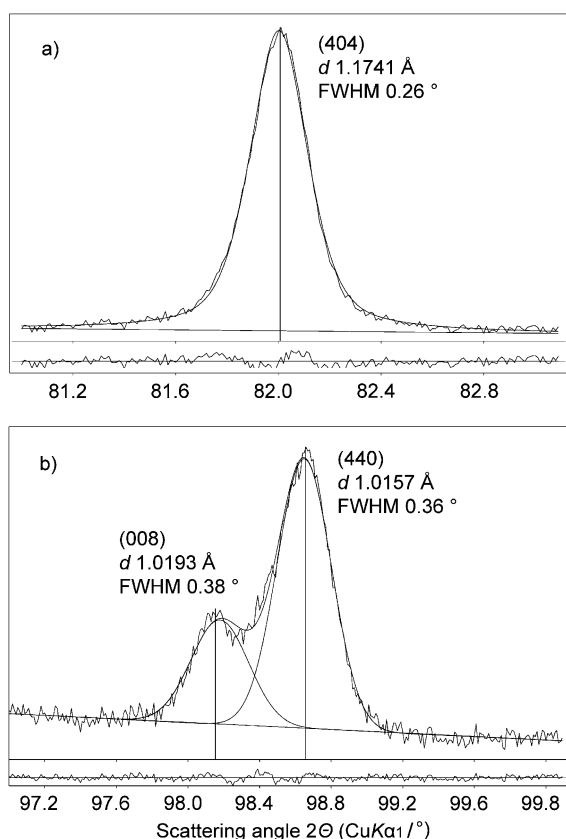


**Figure 2.** Peak fitting results for the two common distortion-sensitive perovskite reflections in the XRD profile of  $\text{KCa}(\text{XeNaO}_6)$ . a) Symmetric unsplit (404) reflection (indexed as (444) in the cubic setting) indicates the lack of angular lattice distortions. b) Two-peak splitting of cubic (800) reflection indicative of the tetragonal symmetry<sup>[5]</sup> of  $\text{KCa}(\text{XeNaO}_6)$ .

formerly reported in the  $^{129}\text{Xe}$  NMR spectra of sodium perxenates; the latter effect has been ascribed to the heteronuclear dipolar coupling between  $^{129}\text{Xe}$  and  $^{23}\text{Na}$  nuclei.<sup>[7]</sup> In that case, however, the line broadening would positively correlate with the Xe–Na distances in the corresponding crystal structures, which is not supported by the experimental data; the NMR spectrum of crystal hydrate  $\text{K}_2\text{Na}_2(\text{XeO}_6) \cdot 8\text{H}_2\text{O}$  taken for reference purposes exhibits very sharp and narrow  $^{129}\text{Xe}$  resonances, in spite of the substantially smaller Xe–Na distance of 3.31 Å relative to the large  $d(\text{Xe}–\text{Na})$  in the perovskites (Table 1). The most plausible explanation for the observed NMR signal broadening is the nanoscale size (50–200 nm) of xenon perovskite crystallites (Supporting Information). That size-dependent broadening of resonances is a known phenomenon in the solid-state NMR of nanoparticles and is related to structural defects and lattice strains occurring at the particle surface.<sup>[8]</sup> Further examination of the  $^{129}\text{Xe}$  NMR spectra reveals one more structure-related feature of  $\text{KCa}(\text{XeNaO}_6)$ : the apparent splitting of the  $^{129}\text{Xe}$  resonance in its spectrum as compared with the isotropic shifts of  $\text{KSr}(\text{XeNaO}_6)$  and  $\text{KBa}(\text{XeNaO}_6)$  (Figure 3). The main resonances between –774 and –770 ppm in all three perovskites can be unambiguously assigned to the symmetric octahedral ( $\text{XeO}_6$ ) environ-

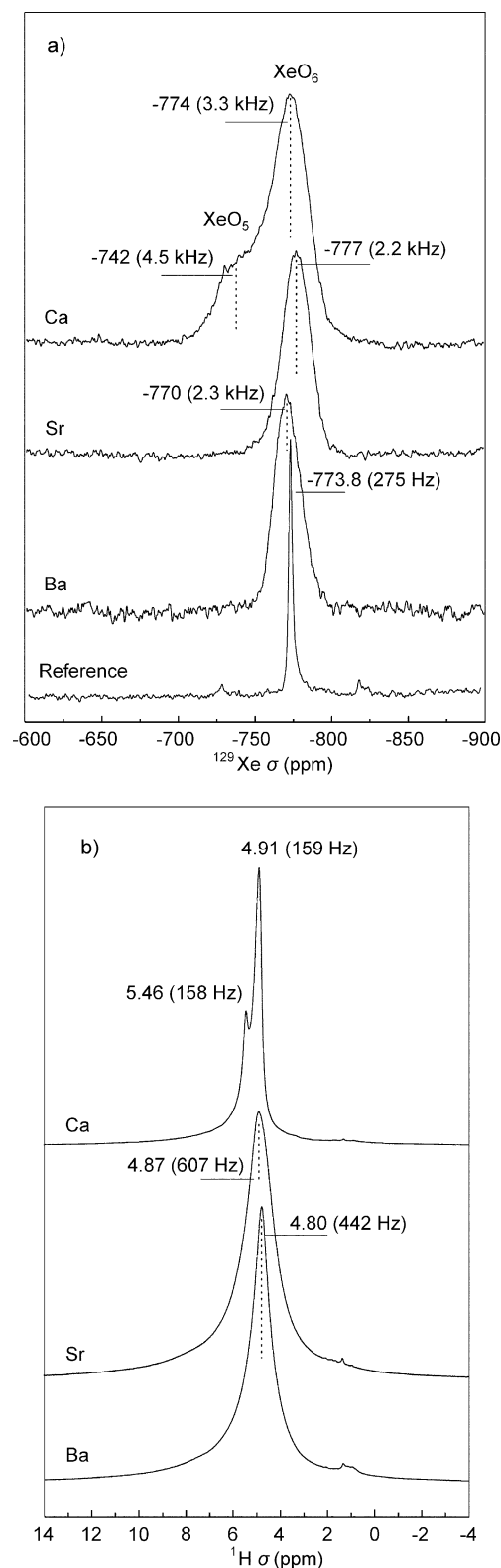


**Figure 3.** a)  $^{129}\text{Xe}$  and b)  $^1\text{H}$  solid-state MAS NMR spectra of perovskites  $\text{KM}(\text{XeNaO}_6)$  where  $\text{M} = \text{Ca}, \text{Sr}, \text{Ba}$ . The full widths at half-maxima (FWHM) of the corresponding resonances are given in the parentheses. The sharp  $^{129}\text{Xe}$  NMR resonance labeled as Reference corresponds to the crystal hydrate  $\text{K}_2\text{Na}_2(\text{XeO}_6) \cdot 8\text{H}_2\text{O}$ .

**Table 1:** Selected structural parameters for  $\text{KM}(\text{XeNaO}_6)$  perovskites (estimated standard deviations are given in parentheses).<sup>[a]</sup>

	Ca	Sr	Ba
Crystal system	Tetragonal	Cubic	Cubic
Space group	$I4/m$	$Fm\bar{3}m$	$Fm\bar{3}m$
$a$ [Å]	5.7500(1)	8.1920(1)	8.3188(2)
$c$ [Å]	8.1558(2)		
$Z$	2	4	4
$V/Z$ [Å <sup>3</sup> ]	134.83(1)	137.44(1)	143.92(1)
$D_x$ [g cm <sup>-3</sup> ]	3.83	4.55	4.92
Tolerance factor	0.956	0.973	1.002
Tilt angle [°]	19.23	0	0
$d(\text{Xe-O})$ [Å]	$2 \times 1.752(9)$ $4 \times 1.746(9)$	$6 \times 1.838(2)$	$6 \times 1.862(2)$
$d(\text{Na-O})$ [Å]	$2 \times 2.326(9)$ $4 \times 2.377(9)$	$6 \times 2.258(2)$	$6 \times 2.298(2)$
$d(\text{Xe-Na})$ [Å]	4.078(1)	4.0960(2)	4.1594(2)

[a] Structural models for the Rietveld refinements were taken from Ref. [5].

ment;<sup>[7]</sup> at the same time, the origin of the high-frequency shoulder at  $-743$  ppm in the spectrum of  $\text{KCa}(\text{XeNaO}_6)$  appears enigmatic. The large difference (31 ppm) between the shifts of the main resonance and the shoulder cannot be assigned to the distortions in the  $(\text{XeO}_6)$  octahedra: the latter would fall well beyond the structurally determined distortion values (Table 1). In comparison, the angular distortions in the  $(\text{XeO}_6)$  octahedron of  $\text{K}_2\text{Na}_2(\text{XeO}_6) \cdot 8\text{H}_2\text{O}$  cover the range of 1.4 degrees, while the Xe–O distances vary from 1.836 to 1.849 Å (Supporting Information). It is worth noting that these distortions do not cause any splitting of the sharp and narrow  $^{129}\text{Xe}$  NMR resonance of  $\text{K}_2\text{Na}_2(\text{XeO}_6) \cdot 8\text{H}_2\text{O}$  (Figure 3). At the same time, it is unlikely that the observed resonance splitting in the spectrum of  $\text{KCa}(\text{XeNaO}_6)$  is associated with the occurrence of five-coordinated xenon owing to oxygen site vacancies. The interrelations between NMR chemical shifts and coordination numbers are well studied for different nuclei,<sup>[9]</sup> and the general trend herein is the NMR shift towards higher frequencies (the downfield one) upon decrease of the coordination number. However, the absolute values of those shifts for the period 4 and 5 elements are much greater; for instance, the gap between the  $^{119}\text{Sn}$  NMR shifts of six- and five-coordinated tin reaches 140 ppm.<sup>[9b]</sup> In that respect, the plausible explanation for the observed  $^{129}\text{Xe}$  resonance splitting is the occurrence of protons residing in the vicinity of framework oxygens or, in other words, the bridging framework hydroxy groups (Figure 1).<sup>[9c]</sup> The compensation of thus acquired charge imbalance can be achieved through insignificant changes in the  $\text{K}^+/\text{Ca}^{2+}$  ratio. The occurrence of the bridging hydroxy group is well corroborated with the results of  $^1\text{H}$  MAS NMR spectroscopy. Figure 3b depicts the  $^1\text{H}$  MAS NMR spectra of the studied perovskites. Besides the common  $^1\text{H}$  resonance at 4.8–4.9 ppm, which can be attributed to the surface hydroxy groups, the spectrum of  $\text{KCa}(\text{XeNaO}_6)$  contains a sharp satellite at 5.46 ppm; the latter can be assigned to the interstitial proton species residing at the bridging oxygen sites. The presence of bridging hydroxy groups in perovskite-type oxides are known to potentially result in protonic

conductivity of the corresponding compounds.<sup>[10]</sup> Unfortunately, the relevant studies of xenon perovskites by means of impedance spectroscopy were largely complicated by their nanoscale size. We could not eliminate the influence of surface hydroxy groups and the presence of unavoidable impurities of amorphous surface carbonate species (Supporting Information), a known problem in the studies of proton conductivity of nanosized oxide perovskites.<sup>[11]</sup>

The xenon perovskites reported herein were synthesized under soft hydrothermal conditions, and their thermal stability is limited to the temperature margins of 360–380 °C (Supporting Information), in concordance with the relatively low thermal stability of xenon–oxygen compounds.<sup>[12]</sup> However, the fact that octavalent xenon can be incorporated into a perovskite framework could provide some new insights into an old mysterious question: the known depletion of atmospheric xenon on Earth (and Mars) relative to argon and krypton, as compared to the composition of carbonaceous chondrite meteorites.<sup>[13]</sup> The latter, being the most primitive presolar substance available for study, are thought to bear the early cosmic noble gas signature.<sup>[14]</sup> The relative depletion of planetary atmospheric xenon cannot be explained simply by its escape into space: xenon is the heaviest among the stable atmospheric gases, and would be expected to be lost later than argon and krypton.<sup>[14]</sup> Among the numerous hypotheses aiming to explain the “missing xenon” paradox, we would like to point out those dealing with the selective uptake of atmospheric noble gases by the silicate minerals early in the history of the Earth. The main silicate phase of the Earth’s interior is generally thought to be  $\text{MgSiO}_3$  perovskite (bridgmanite),<sup>[15]</sup> the mineral containing silicon in an octahedral coordination.  $\text{MgSiO}_3$  perovskite can preferentially take up gaseous argon, likely through a mechanism involving the insertion of neutral Ar atoms into the oxygen vacancies or interstices of the  $\text{MgSiO}_3$  perovskite framework. Thus, observed argon uptake was found to reach 1 wt.% at the pressure of 25 GPa and temperature between 1600 and 1800 °C.<sup>[14]</sup>

At the same time, there is evidence for the high solubility of xenon in the silicate systems at elevated temperatures and pressures.<sup>[16]</sup> The incorporation of Xe has been attributed to the direct intercalation of neutral Xe atoms into oxygen vacancies, substitution of Xe for Si, and formation of tetrahedral xenon oxide species.<sup>[16]</sup> In particular, the extremely high solubility of Xe in the Xe– $\text{SiO}_2$  system has been shown to occur at 0.7–1.5 GPa pressure and the temperature of 1500–1750 °C: the  $P$ – $T$  conditions characteristic of the deep Earth’s crust.<sup>[16b]</sup> The observed phenomenon has been attributed to the possible formation of xenon-containing silicate phases. Sanloup et al.<sup>[16b]</sup> have reported an unidentified xenon-bearing silicate stable up to 2.14 GPa which contains at least 4 wt.% of Xe in the quenched state. That silicate–xenon phase has a body-centered cubic cell with the lattice parameter of 8.03 Å. At that point, the above given parameter, along with the  $I$ -centered Bravais lattice, are well consistent with the unit-cell data for the high-pressure polymorph of  $\text{ReO}_3$ .<sup>[17]</sup> a prototypic double perovskite whose formula can be represented as  $(\square)_2(\text{ReReO}_6)$ , where  $(\square)$  denotes a vacancy at the 12-coordinate  $A$ -site. Although

there are no experimental reports on the stability of  $\text{Xe}^{\text{VIII}}$  compounds at high  $P$ – $T$  conditions, a recent computational study provides evidence that xenon loses its inertness at the high pressures, allowing the pressure-induced formation of xenon oxides.<sup>[18]</sup> Therefore, we can assume that the high  $P$ – $T$  xenon–silicate phase reported by Sanloup et al.<sup>[16b]</sup> might represent a new form of xenon incorporation into silica-based systems: by direct substitution of Si for Xe in  $\text{ReO}_3$ -type double perovskite structure. The proximity of the ionic radius of octahedrally coordinated  $\text{Xe}^{\text{VIII}}$  (0.48 Å) to that of octahedral  $\text{Si}^{\text{IV}}$  (0.40 Å)<sup>[4]</sup> suggests that octavalent xenon can directly substitute for octahedrally coordinated silicon in hyperbaric silicate frameworks, including silicate perovskites such as hypothetical  $\text{ReO}_3$ -type  $(\square)_2(\text{XeSiO}_6)$  or Xe-substituted  $\text{MgSiO}_3$  perovskite,  $\text{Mg}_{2-x}(\text{Si}_{1-x}\text{Xe}_x\text{O}_3)$ . Since  $\text{MgSiO}_3$  perovskite is accepted to be the dominant silicate phase in the Earth's interior, even insignificant incorporation of Xe into  $\text{MgSiO}_3$  frameworks could provide an explanation for the observed xenon depletion in the Earth's atmosphere.

The ability of xenon(VIII) to form stable inorganic frameworks might inspire new insights into the chemistry of that noble gas:  $\text{Xe}^{\text{VIII}}$  can be considered a crystal chemical counterpart of group 4–5 transition metals (Ti, Nb and Ta) so one can expect the emergence of  $\text{Xe}^{\text{VIII}}$  compounds that could replicate the rich crystal chemistry of titanium, niobium, and tantalum oxides.

## Experimental Section

Anhydrous sodium perxenate,  $\text{Na}_4\text{XeO}_6$ , was synthesized following the previously published procedures.<sup>[19]</sup> Reagent grade KOH, NaOH,  $\text{Ca}(\text{NO}_3)_2 \cdot 4\text{H}_2\text{O}$ ,  $\text{Sr}(\text{NO}_3)_2$ , and  $\text{Ba}(\text{NO}_3)_2$  were used as supplied. Deionized water (18 MΩ) was used in all procedures.

Suspension 1: 1 mmol of either  $\text{Ca}(\text{NO}_3)_2 \cdot 4\text{H}_2\text{O}$ ,  $\text{Sr}(\text{NO}_3)_2$ , or  $\text{Ba}(\text{NO}_3)_2$  was dissolved in 1 mL of water and mixed with 5 mL of 10 N KOH. Suspension 2: 100 mg of NaOH was dissolved in 5 mL of 10 N KOH. In that solution, 1 mmol of  $\text{Na}_4\text{XeO}_6$  was suspended. Suspension 1 was then mixed with suspension 2 in a 50 mL Teflon-lined autoclave. The autoclave was sealed and held at 170 °C for 24 h. Upon cooling to room temperature, the resultant reaction mixture was transferred into a 100 mL polyethylene beaker. The white precipitates of either  $\text{KCa}(\text{XeNaO}_6)$ ,  $\text{KSr}(\text{XeNaO}_6)$ , or  $\text{KBa}(\text{XeNaO}_6)$  were washed 10 times with 70 mL portions of water, transferred on filter paper, and air-dried at 60 °C for 1 h. Yields:  $\text{KCa}(\text{XeNaO}_6)$  = 292 mg (88%),  $\text{KSr}(\text{XeNaO}_6)$  = 235 mg (62%),  $\text{KBa}(\text{XeNaO}_6)$  = 240 mg (56%).

Analytical calculations for  $\text{KCa}(\text{XeNaO}_6)$  ( $M$  = 329.45): K 11.87, Ca 12.17, Na 6.98; found (ICP-OES): K 13.67, Ca 11.07, Na 6.22 wt. %. EDX: atomic ratio of K/Ca/Xe/Na is 1.07/0.95/0.99/0.98.

Analytical calculations for  $\text{KSr}(\text{XeNaO}_6)$  ( $M$  = 376.99): K 10.37, Sr 23.24, Na 6.10; found (ICP-OES): K 10.83, Sr 23.17, Na 5.98 wt. %. EDX: atomic ratio of K/Sr/Xe/Na 1.08/1.02/1.01/0.92.

Analytical calculations for  $\text{KBa}(\text{XeNaO}_6)$  ( $M$  = 426.70): K 9.16, Ba 32.18, Na 5.39; found (ICP-OES): K 9.38, Ba 32.20, Na 3.78 wt. %. EDX: atomic ratio of K/Ba/Xe/Na 1.10/1.19/0.93/0.72.

$\text{K}_2\text{Na}_2\text{XeO}_6 \cdot 8\text{H}_2\text{O}$ . 500 mg of anhydrous  $\text{Na}_4\text{XeO}_6$  was suspended in 10 mL of 5 N KOH at 80 °C in plastic syringe. The suspension was cooled to room temperature, transferred into refrigerator and held at 4 °C overnight. The resultant colorless crystals of  $\text{K}_2\text{Na}_2\text{XeO}_6 \cdot 8\text{H}_2\text{O}$  were extracted by decantation of the parent solution, transferred on filter paper, rinsed with 2 mL of 0.5 N KOH and air-dried at room temperature. Yield: 270 mg (54%). Analytical calculations for

$\text{K}_2\text{Na}_2\text{XeO}_6 \cdot 8\text{H}_2\text{O}$  ( $M$  = 495.58): K 15.78, Na 9.28; found (ICP-OES): K 15.96, Na 9.17 wt. %.

Rietveld Refinement details, crystallographic data, EDX spectra, SEM photo, FTIR spectra, TGA-DSC data for  $\text{KCa}(\text{XeNaO}_6)$ ,  $\text{KSr}(\text{XeNaO}_6)$ ,  $\text{KBa}(\text{XeNaO}_6)$ , data collection details, and structural parameters of  $\text{K}_2\text{Na}_2\text{XeO}_6 \cdot 8\text{H}_2\text{O}$  are provided in the Supporting Information. Further details on the crystal structure investigations may be obtained from the Fachinformationszentrum Karlsruhe, 76344 Eggenstein-Leopoldshafen, Germany (fax: (+49) 7247-808-666; e-mail: crysdata@fiz-karlsruhe.de), on quoting the depository number CSD-429919.

## Acknowledgements

This research was supported by a research grant 3.37.222.2015 awarded by the Saint-Petersburg State University. The authors thank the X-ray Diffraction Center, the Center for Magnetic Resonance and the Resource center for Geo-Environmental Research and Modeling of SPSU for XRD, NMR and EDX measurements.

**Keywords:** framework structures · nanoparticles · oxides · perovskites · xenon

**How to cite:** *Angew. Chem. Int. Ed.* **2015**, *54*, 14340–14344  
*Angew. Chem.* **2015**, *127*, 14548–14552

- a) J. Haner, G. J. Schrobilgen, *Chem. Rev.* **2015**, *115*, 1255–1295; b) A. Bauzá, A. Frontera, *Angew. Chem. Int. Ed.* **2015**, *54*, 7340–7343; *Angew. Chem.* **2015**, *127*, 7448–7451.
- a) M. T. Anderson, K. B. Greenwood, G. A. Taylor, K. R. Poeppelmeier, *Prog. Solid State Chem.* **1993**, *22*, 197–233; b) K. D. Karlin, D. B. Mitzi, *Prog. Inorg. Chem.* **1999**, *48*, 1–121; c) M. A. Peña, J. L. G. Fierro, *Chem. Rev.* **2001**, *101*, 1981–2017; d) R. H. Mitchell, *Perovskites modern and ancient*, Almaz Press, Thunder Bay, Ontario, **2002**, pp. 1–318; e) R. E. Schaak, T. E. Mallouk, *Chem. Mater.* **2002**, *14*, 1455–1471; f) B. V. Lotsch, *Angew. Chem. Int. Ed.* **2014**, *53*, 635–637; *Angew. Chem.* **2014**, *126*, 647–649.
- S. Vasala, M. Karppinen, *Prog. Solid State Chem.* **2015**, *43*, 1–36.
- R. D. Shannon, *Acta Crystallogr. Sect. A* **1976**, *32*, 751–767.
- a) M. Gateshki, J. M. Igartua, E. Hernández-Bocanegra, *J. Phys. Condens. Matter* **2003**, *15*, 6199–6217; b) Q. Zhou, B. J. Kennedy, C. J. Howard, M. M. Elcombe, A. J. Studer, *Chem. Mater.* **2005**, *17*, 5357–5365.
- a) V. M. Goldschmidt, *Naturwissenschaften* **1926**, *14*, 477–485; b) C. J. Howard, B. J. Kennedy, P. M. Woodward, *Acta Crystallogr. Sect. B* **2003**, *59*, 463–471.
- M. A. M. Forgeron, R. E. Wasylshen, M. Gerken, G. J. Schrobilgen, *Inorg. Chem.* **2007**, *46*, 3585–3592.
- a) F. V. Mikulec, M. Kuno, M. Bennati, D. A. Hall, R. G. Griffin, M. G. Bawendi, *J. Am. Chem. Soc.* **2000**, *122*, 2532–2540; b) L. Protesescu, A. J. Rossini, D. Kriegner, M. Valla, A. de Kergommeaux, M. Walter, K. V. Kravchik, M. Nachttegaal, J. Stangl, B. Malaman, P. Reiss, A. Lesage, L. Emsley, C. Copéret, M. V. Kovalenko, *ACS Nano* **2014**, *8*, 2639–2648.
- a) J. M. Cocciantelli, K. S. Suh, J. Sénégas, J. P. Doumerc, J. L. Soubeyroux, M. Pouchard, P. Hagenmüller, *J. Phys. Chem. Solids* **1992**, *53*, 51–55; b) L. Buannic, F. Blanc, D. S. Middlemiss, C. P. Grey, *J. Am. Chem. Soc.* **2012**, *134*, 14483–14498; c) I. Oikawa, M. Ando, Y. Noda, K. Amezawa, H. Kiyono, T. Shimizu, M. Tansho, H. Maekawa, *Solid State Ionics* **2011**, *192*, 83–87.
- a) A. S. Nowick, Y. Du, *Solid State Ionics* **1995**, *77*, 137–146; b) Ph. Colomban, *Ann. Chim. Sci. Mater.* **1999**, *24*, 1–18.

- [11] Ph. Colomban, C. Tran, O. Zaafrani, A. Slodczyk, *J. Raman Spectrosc.* **2013**, *44*, 312–320.
- [12] a) B. Jaselskis, J. L. Huston, T. M. Splitter, *J. Am. Chem. Soc.* **1969**, *91*, 2149–2150; b) V. Ya. Mishin, I. S. Kirin, V. K. Isupov, Yu. K. Gusev, *Zh. Neorg. Khim.* **1971**, *16*, 51–55; c) L. Khriachtchev, K. Isokoski, A. Cohen, M. Räsänen, R. B. Gerber, *J. Am. Chem. Soc.* **2008**, *130*, 6114–6118; d) M. Gerken, G. J. Schrobilgen, *Inorg. Chem.* **2002**, *41*, 198–204; e) M. D. Moran, D. S. Brock, H. P. A. Mercier, G. J. Schrobilgen, *J. Am. Chem. Soc.* **2010**, *132*, 13823–13829; f) D. S. Brock, H. P. A. Mercier, G. J. Schrobilgen, *J. Am. Chem. Soc.* **2013**, *135*, 5089–5104.
- [13] a) R. O. Pepin, D. Porcelli, *Rev. Mineral. Geochem.* **2002**, *47*, 191–246; b) D. S. Brock, G. J. Schrobilgen, *J. Am. Chem. Soc.* **2011**, *133*, 6265–6269.
- [14] S. S. Shcheka, H. Keppler, *Nature* **2012**, *490*, 531–534.
- [15] O. Tschauner, C. Ma, J. R. Beckett, C. Prescher, V. B. Praka-penka, G. R. Rossman, *Science* **2014**, *346*, 1100–1102.
- [16] a) T. Shibata, E. Takahashi, J.-I. Matsuda, *Geochim. Cosmo-chim. Acta* **1998**, *62*, 1241–1253; b) C. Sanloup, R. J. Hemley, H. Mao, *Geophys. Res. Lett.* **2002**, *29*, 1883; c) B. C. Schmidt, H. Keppler, *Earth Planet. Sci. Lett.* **2002**, *195*, 277–290; d) C. Sanloup, B. C. Schmidt, E. M. C. Perez, A. Jambon, E. Gregory-anz, M. Mezouar, *Science* **2005**, *310*, 1174–1177; e) C. Sanloup, B. C. Schmidt, G. Gudfinnsson, A. Dewaele, M. Mezouar, *Geochim. Cosmochim. Acta* **2011**, *75*, 6271–6284.
- [17] J.-E. Jørgensen, J. D. Jørgensen, B. Batlogg, J. P. Remeika, J. D. Axe, *Phys. Rev. B* **1986**, *33*, 4793–4798.
- [18] Q. Zhu, D. J. Jung, A. R. Oganov, C. W. Glass, C. Gatti, A. O. Lyakhov, *Nat. Chem.* **2013**, *5*, 61–65.
- [19] E. H. Appelman, *Inorg. Synth.* **1968**, *11*, 210–213.

Received: July 20, 2015

Published online: October 2, 2015